Minimax Model Predictive Operation
Control of Microgrids [⋆]

Christian A. Hans [∗] **Vladislav Nenchev** [∗,∗∗] **Jörg Raisch** [∗,∗∗∗]
Carsten Reincke-Collon [∗∗∗∗]

[∗] *Technische Universität Berlin, Germany,*
{hans,nenchev,raisch}@control.tu-berlin.de
[∗∗] *Boston University, USA*
[∗∗∗] *Max-Planck-Institut für Dynamik komplexer*
technischer Systeme, Germany
[∗∗∗∗] *Younicos AG, Germany, reincke-collon@younicos.com*

Abstract: Due to the steady growth of decentralised distributed generation, the operational management of small, local electricity networks (microgrids) is becoming an increasing challenge to meet: How to provide an operational control for microgrids with a high share of renewable energy sources (RES) that is robust to perturbations? In this paper we address an optimal control problem (OCP) that maintains all of the stated properties in the presence of an uncertain load and RES infeed in islanded operation. Assuming that the uncertainty is within a bounded region along a given load and RES trajectory prediction, the problem is posed as a worst-case hybrid OCP, where the RES output can be curtailed. We propose a minimax (MM) model predictive control (MPC) scheme that adjusts according to the present uncertainty and can be formulated as a mixed-integer linear program (MILP) and solved numerically online.

Keywords: Energy management systems; Energy storage; Integer programming; Optimal control; Optimal power flow; Predictive control; Unit commitment.

1. INTRODUCTION

Microgrids (MGs) are small, local energy networks that include storage devices, thermal and renewable generation. Such energy supply solutions are expected to cope with the steady growth of RES by matching consumption and generation on a local scale. This reduces the load flow over long distances. Also the reliability of supply can be increased by running the grid autonomously in islanded mode as stated by Lopes et al. (2006). Small grids that are (due to geographical or infrastructural circumstances) always operated in islanded mode also fit into the class of microgrids. During islanded operation, the storage or the thermal generator (or both in parallel) form the grid providing voltage and frequency.

As the initial investment of RES is much higher than for thermal generators it is desired to maximise the infeed of the installed RES. In some configurations, the installed RES power may exceed the nominal load to keep its share high even in times of low wind or irradiation. In times of high RES infeed, the energy surplus can be used to charge storage facilities. In case that the storage devices are completely charged or a power limit is reached, the RES infeed can be limited (or curtailed).

In order to maximise the RES infeed and save as much fuel (needed for the thermal generation) as possible, the operation of microgrids is optimised by adapting the power set points of the units. Due to the relatively large time constants in operation, it is sufficient to repeat the optimisation on a time scale of several minutes, to adapt with respect to the difference between the forecasted and measured states. Hence, MPC is a natural approach to adopt.

Lately, model predictive operation of power systems has received considerable attention. Arnold et al. (2009) proposed a MPC strategy for a given perfect forecast, based on the energy hub framework of Heussen et al. (2010). This framework was also used by Zafra-Cabeza et al. (2010) for a risk based economic planning of power systems. An alternative economic scheduling, where no forecast uncertainties were assumed was proposed by Parisio and Glielmo (2011). The suggested MPC approach took into account the on and off switching of the machines and was formulated as a MILP. In unit commitment many robust optimisation approaches were suggested. Bertsimas et al. (2013) combined MILP with a stochastic approach for a reliability constrained problem and proposed an adaptive strategy to cope with uncertainties. A unified stochastic and robust approach was proposed by Zhao and Guan (2013) using existing forecasts of load and RES infeed. A comparison of a minimax and a stochastic optimisation was given by Jiang et al. (2013).

Broadly speaking, there are two classes of approaches. One takes into account the storage dynamics but neglects forecast uncertainties. The other consists of unit commitment approaches which typically allow uncertainties in forecasts but do not consider the dynamics of storage units. To the

best knowledge of the authors, the possibility of limiting the RES infeed in order to obtain a robust MPC scheme has not yet been taken into account by any of them.

Our main contribution is the combination of the MPC approach for dynamical systems with a minimax optimisation, where a limitation of the RES is possible. The proposed scheme takes into account possible disturbances on the power and the stored energy, leading to a control where no unit constraints are violated in the presence of uncertainties.

The outline of the paper is as follows. First, we introduce notation and summarise some facts from graph theory and DC power flow. Several assumptions are made and the model with its constraints is described and used in our problem formulation. In Section 3, a certainty equivalent and a minimax solution for the problem are proposed. Both approaches are compared in a numerical case study.

2. PROBLEM FORMULATION

In this section, the OCP of minimising a scalar cost function that includes minimising the thermal generator infeed and maximising the RES infeed in the presence of uncertain forecasts is described. We start by introducing some notation.

Notation: We define the sets $\mathbb{R}_+ = \{x \in \mathbb{R} | x > 0\}$ and $\mathbb{R}_{0+} = \{x \in \mathbb{R} | x \geq 0\}$. Boolean variables are denoted by $\mathbb{B} = \{0, 1\}$. The cardinality of a set $\mathcal{V}$ is denoted by $|\mathcal{V}|$. Let $\text{diag}(a_1, \ldots, a_n)$ denote the $n \times n$ diagonal matrix with diagonal entries a_i, $i = 1, \ldots, n$ and $\mathbf{I}_n$ the identity matrix. Furthermore, $\mathbf{0}_{n \times m}$ is the $n \times m$ matrix of all zeros and $\mathbf{1}_{n \times m}$ the matrix of ones. The $n \times 1$ zero vector is denoted by $\mathbf{0}_n$ and the vector of ones by $\mathbf{1}_n$.

2.1 Preliminaries

A network is modelled as a weighted, undirected graph, i.e., a triple $\mathcal{G} = (\mathcal{V}, \mathcal{E}, \mathcal{W})$, where $\mathcal{V} = \{1, \ldots, v\}$ is the set of nodes, $\mathcal{E} \subseteq \mathcal{V} \times \mathcal{V}$ the set of edges with $|\mathcal{E}| = e$ and $\mathcal{W} : \mathcal{E} \to \mathbb{R}_+$ a weight function. The graph can be represented algebraically by its adjacency matrix $\mathcal{Y}$ with entries

$$y_{ij} = \begin{cases} \mathcal{W}((i,j)) & \text{if } (i,j) \in \mathcal{E} \\ 0 & \text{otherwise.} \end{cases}$$

The set of nodes is partitioned into five subsets $\mathcal{V}_\mathcal{L}$, $\mathcal{V}_\mathcal{R}$, $\mathcal{V}_\mathcal{S}$, $\mathcal{V}_\mathcal{G}$ and $\mathcal{V}_\mathcal{N}$, where the elements of $\mathcal{V}_\mathcal{L}$ represent the connected loads, the elements of $\mathcal{V}_\mathcal{R}$ the RES, the elements of $\mathcal{V}_\mathcal{S}$ the storage units, the elements of $\mathcal{V}_\mathcal{G}$ the thermal generators and the elements of $\mathcal{V}_\mathcal{N}$ the passive nodes where no equipment is connected. Note that the utility grid in this framework is represented by a thermal generator with high nominal power as part of $\mathcal{V}_\mathcal{G}$. Let $|\mathcal{V}_\mathcal{L}| = l$, $|\mathcal{V}_\mathcal{R}| = r$, $|\mathcal{V}_\mathcal{S}| = s$, $|\mathcal{V}_\mathcal{G}| = g$ and $|\mathcal{V}_\mathcal{N}| = n$. Power lines are represented by the edges (i, j), $i \neq j$ that connect two different nodes. By choosing for each edge $(i, j) \in \mathcal{E}$ a unique number $d \in [1, |\mathcal{E}|] \subset \mathbb{N}$, the node-edge incidence matrix $\mathcal{B} \in \mathbb{R}^{v \times e}$ is defined element wise as $b_{id} = 1$, if node i is the sink of edge d, $b_{id} = -1$, if i is the source of edge d and $b_{id} = 0$ else.

Power Flow: If the voltage differences (in angle and amplitude) are small and the line resistances are negligible (lossless lines), the linearised DC power flow equations can be used as stated by Purchala et al. (2005). The power flow $P_\mathcal{E} \in \mathbb{R}^e$ over the (inductive) lines is then calculated with the phase angles of the nodes, $\Theta \in \mathbb{R}^v$ by

$$P_\mathcal{E} = \text{diag}(y_{ij}) \mathcal{B}^T \Theta,$$

where $\text{diag}(y_{ij}) \in \mathbb{R}^{e \times e}$ is the diagonal matrix of all non-zero edge weights and $\mathcal{B}$ is the node-edge incidence matrix. Power flow between the nodes can be calculated by the linearised (DC power flow) model with $P_\mathcal{V} = \mathbf{Y}\Theta$, where $\mathbf{Y} \in \mathbb{R}^{v \times v}$ is the Laplacian matrix with $\mathbf{Y} = \mathcal{B} \text{diag}(y_{ij}) \mathcal{B}^T$:

$$P_\mathcal{V} = \begin{pmatrix} p_1 \\ p_2 \\ \vdots \\ p_v \end{pmatrix} = \begin{pmatrix} \sum_{j=2}^v y_{1j} & \cdots & -y_{1v} \\ -y_{21} & \cdots & -y_{2v} \\ \vdots & \ddots & \vdots \\ -y_{v1} & \cdots & \sum_{j=1}^{v-1} y_{vj} \end{pmatrix} \begin{pmatrix} \theta_1 \\ \theta_2 \\ \vdots \\ \theta_v \end{pmatrix}. \quad (1)$$

In the following, we assume that the graph is connected, i.e. there is a path from every node to all the other nodes. Then, the Laplacian has the rank $v - 1$. Therefore, we have to fix one phase angle in order to obtain the rest of the angles as a function of the power values. This is possible as the power flow only depends on the phase angle differences and can be achieved with the transformation

$$\Theta' = \underbrace{\begin{pmatrix} \mathbf{I}_{(v-1)} & -\mathbf{1}_{(v-1)} \\ \mathbf{0}_{(v-1)}^T & 1 \end{pmatrix}}_{\mathbf{T}} \Theta = \begin{pmatrix} \theta_1 - \theta_v \\ \vdots \\ \theta_{(v-1)} - \theta_v \\ \theta_v \end{pmatrix}. \quad (2)$$

As each row of a Laplacian sums up to zero, merging (1) and the inverse transformation (2) leads to

$$P_\mathcal{V} = \mathbf{Y}\Theta = \mathbf{Y}\mathbf{T}^{-1}\Theta' = \begin{pmatrix} \tilde{\mathbf{Y}} & \mathbf{0}_{(v-1)} \\ b^T & 0 \end{pmatrix} \Theta',$$

or with $P_\mathcal{V}^T = (\tilde{P}_\mathcal{V}^T, p_v)^T$ and $\Theta'^T = (\tilde{\Theta}'^T, \theta_v)^T$, where $\tilde{P}_\mathcal{V} \in \mathbb{R}^{(v-1)}$, $\tilde{\Theta}' \in \mathbb{R}^{(v-1)}$ and $p_v \in \mathbb{R}$

$$\begin{pmatrix} \tilde{P}_\mathcal{V} \\ p_v \end{pmatrix} = \begin{pmatrix} \tilde{\mathbf{Y}} & \mathbf{0}_{(v-1)} \\ b^T & 0 \end{pmatrix} \begin{pmatrix} \tilde{\Theta}' \\ \theta_v \end{pmatrix}. \quad (3)$$

The angle $\theta_v \in [-\pi, \pi)$ is a constant, $\tilde{\mathbf{Y}} \in \mathbb{R}^{(v-1) \times (v-1)}$ is a nonsingular matrix and $b \in \mathbb{R}^{(v-1)}$ a vector. As $\det(\tilde{\mathbf{Y}}) \neq 0$ we can invert the matrix and derive $\tilde{\Theta}' = \tilde{\mathbf{Y}}^{-1}\tilde{P}_\mathcal{V}$. Thus, the relative phase angles are $\Theta' = ((\tilde{\mathbf{Y}}^{-1}\tilde{P}_\mathcal{V})^T, \theta_v)^T$ and the power flow over the edges can be calculated with $\Theta = \mathbf{T}^{-1}\Theta'$ and (3) by

$$P_\mathcal{E} = \text{diag}(y_{ij}) \mathcal{B}^T \underbrace{\mathbf{T}^{-1} \begin{pmatrix} \tilde{\mathbf{Y}}^{-1}\tilde{P}_\mathcal{V} \\ \theta_v \end{pmatrix}}_{\Theta}. \quad (4a)$$

We also have to add the equality constraint obtained from the last row of (3), given by

$$p_v = b^T \tilde{\mathbf{Y}}^{-1}\tilde{P}_\mathcal{V}, \quad (4b)$$

which ensures that the sum of all generated and consumed power equals zero. With (4) we can now calculate the power flow over the edges by the power injected or consumed at every node. With the preliminaries stated, we now continue with the assumptions that are made throughout this work.

2.2 Assumptions

In the following we assume that

- electrical devices connected to the grid are capable of running autonomously for several minutes, such that it is sufficient to solve the OCP on the same time scale;
- the storage devices and the thermal generators can form the grid and run as voltage sources providing frequency and voltage; if they run in parallel they share the variations in power coming from the RES and the load;
- no communication failures occur; also the communication delay is assumed to be negligible compared to the sampling time of the operation control;
- the voltage amplitude is constant, the voltage angle differences small and the line resistance is negligible (i.e. we can use the DC power flow equations); the error introduced by this simplification is small compared to the uncertainty that comes from the load and the RES infeed;
- reactive power can be neglected (for simplicity); hence, the line limits are only approximately accounted for;
- forecasts for the load and RES infeed are available in the form of time varying lower and upper bounds.

2.3 Modelling and constraints

For each time step $k \in [0, K] \subset \mathbb{N}$, with the sampling time $t_S \in \mathbb{R}_+$, typically in the domain of minutes, a dynamic state vector $x(k)$, and for $k \in [0, K-1] \subset \mathbb{N}$ a real-valued input $u(k)$, a boolean input $\Delta(k)$ and a disturbance $w(k)$ are given by

$$
\begin{aligned}
x(k) &= E_{\mathcal{S}}(k) \\
u(k) &= \left(P_{\mathcal{G}}^T(k), P_{\mathcal{S}}^T(k), P_{\mathcal{R}}^T(k)\right)^T \\
\Delta(k) &= \left(\Delta_{\mathcal{G}}^T(k), \Delta_{\mathcal{S}}^T(k), \Delta_{\mathcal{R}}^T(k)\right)^T \\
w(k) &= \left(w_{\mathcal{L}}^T(k), w_{\mathcal{R}}^T(k)\right)^T, \text{ where}
\end{aligned}
\tag{5}
$$

- $E_{\mathcal{S}}(k) \in \mathbb{R}_{0+}^s$ is the stored energy in every node of $V_{\mathcal{S}}$;
- $u(k)$ denotes the power of the thermal generation units $P_{\mathcal{G}}(k) \in \mathbb{R}_{0+}^g$, the storage devices $P_{\mathcal{S}}(k) \in \mathbb{R}^s$ and the renewable energy sources $P_{\mathcal{R}}(k) \in \mathbb{R}_{0+}^r$;
- $w_{\mathcal{L}}(k) \in \mathbb{R}^l$ is the bounded variation of the load, $w_{\mathcal{R}}(k) \in \mathbb{R}^r$ is the (also bounded) disturbance emerging due to fluctuation of the RES;
- $\Delta_{\mathcal{G}}(k) \in \mathbb{B}^g$ indicates which thermal unit is currently in operation; similarly $\Delta_{\mathcal{S}}(k) \in \mathbb{B}^s$ and $\Delta_{\mathcal{R}}(k) \in \mathbb{B}^r$ indicate which storage unit or RES is running.

Note that $\Delta(k)$ and $u(k)$ are control variables that share the dependence $\Delta_i(k) = 0 \Rightarrow u_i(k) = 0$.

The fluctuations are assumed to be bounded by $\hat{w}^{\min}(k)$ and $\hat{w}^{\max}(k) \in \mathbb{R}^{(l+r)}$ for any time step k, i.e.

$$
\hat{w}^{\min}(k) \leq w(k) \leq \hat{w}^{\max}(k).
\tag{6}
$$

Power limits: We introduce a virtual slack. The resulting power of this slack is distributed among all thermal generators and storage devices. They de- or increase their power in order to balance the variation of the load and the renewable infeed, respectively. This power sharing is controlled in a decentralised manner as in Schiffer et al. (2012). As the valuation of all disturbances are assumed to be known, the variations can be distributed directly to all running thermal generators and storage units without the need for communication through the frequency. The factors of the power sharing are chosen such that each generator and storage device provides slack power according to its nominal power. The vector $P_{\mathcal{H}} = (P_{\mathcal{G}}^{N^T} \ P_{\mathcal{S}}^{N^T} \ \mathbf{0}_r^T)^T$ with $P_{\mathcal{G}}^N \in \mathbb{R}_{0+}^g$, $P_{\mathcal{S}}^N \in \mathbb{R}_{0+}^s$ contains these nominal power values. As only running machines can de- or increase their power, we define the vector of shared variations $(\mathbf{H}(\Delta)w(k))$ with

$$
\mathbf{H}(\Delta) = \frac{-1}{P_{\mathcal{H}}^T \Delta(k)} \text{diag}(P_{\mathcal{H}}) \Delta(k) \mathbf{1}_{r+l}^T.
\tag{7}
$$

$H_i \leq 0, \forall H_i(\Delta) \in \mathbf{H}(\Delta)$ as the units have to increase their power if the load or the RES power decreases and vice versa. The total power of machine i is given by the sum of the set points $u_i(k)$ and the variations $(\mathbf{H}(\Delta)w(k))_i$. It has to comply with the limits of the machine if it is enabled. If a unit i is disabled, its power infeed is set to zero by the corresponding $\Delta_i(k)$. Thus, the power that the machines deliver or consume at time k corresponds to $u(k) + \mathbf{H}(\Delta)w(k)$ with

$$
\text{diag}(u^{\min})\Delta(k) \leq u(k) + \mathbf{H}(\Delta)w(k) \leq \text{diag}(u^{\max})\Delta(k),
\tag{8}
$$

where $u^{\min}$, $u^{\max} \in \mathbb{R}^{g+s+r}$.

The System dynamics of the storage units are described by

$$
x(k+1) = \mathbf{A}x(k) + \mathbf{B}\left(u(k) + \mathbf{H}(\Delta)w(k)\right), \ x(0) = x_0, \tag{9}
$$

with $\mathbf{A} = \mathbf{I}_s$ and $\mathbf{B} = -t_S\left(\mathbf{0}_{s \times g}, \mathbf{I}_s, \mathbf{0}_{s \times r}\right)$. As storage units can only contain a certain amount of energy, the states are bounded by $x^{\min}$, $x^{\max} \in \mathbb{R}_{0+}^s$ such that

$$
x^{\min} \leq x(k) \leq x^{\max} \ \forall k \in [1, K].
\tag{10}
$$

The DC power flow between the nodes is given by the equations stated in Section 2.1. The generated / consumed power at every node in the network is captured by

$$
P_{\mathcal{V}}(k) = \begin{pmatrix} u(k) + \mathbf{H}(\Delta)w(k, u) \\ w_{\mathcal{L}}(k) \\ P_{\mathcal{N}} \end{pmatrix} = \begin{pmatrix} \tilde{P}_{\mathcal{V}}(k) \\ p_v(k) \end{pmatrix}.
$$

The passive network nodes (where no power is generated or consumed) are defined as $P_{\mathcal{N}} = \mathbf{0}_n$. They were introduced to represent the structure of the grid in an intuitive way and could be reduced in a later step. The power flow over the lines, defined in (4) is limited by

$$
P_{\mathcal{E}}^{\min} \leq P_{\mathcal{E}}(k) \leq P_{\mathcal{E}}^{\max},
\tag{11}
$$

for $P_{\mathcal{E}}^{\min}, P_{\mathcal{E}}^{\max} \in \mathbb{R}^e$. To ensure that the generated meets the consumed power (4b) must also hold $\forall k \in [0, K-1]$.

Short circuit power is taken as a measure for the strength of a grid. It is used instead of the spinning reserve, which is a common indicator for the capability to react to transient events. Droop controlled inverters have a virtual spinning reserve that can be much higher than that of a generator at the same power rating. Thus the spinning reserve in microgrids with voltage source inverters is not connected directly to the behaviour during transient events any more. Hence, it is more beneficial to use the short circuit power, which is limited by the hardware of both, inverter and classical generator. Even though the short circuit power

depends on the transmission lines and varies between the nodes, it still can be used as an indicator. This short circuit power $p^{\mathrm{sc}} \in \mathbb{R}_{0+}$ must be provided in every instant k. The boolean vector $\Delta(k)$ again indicates which machine is connected and therefore provides its service to the grid. The maximum short circuit power that the machines can deliver is given by $P_{\mathcal{U}}^{\mathrm{sc}} \in \mathbb{R}_{0+}^{(g+s+r)}$ and has to fulfil

$$(P_{\mathcal{U}}^{\mathrm{sc}})^T \Delta(k) \geq p^{\mathrm{sc}}, \forall k \in [0, K-1]. \tag{12}$$

2.4 Problem formulation

We define a cost function that penalises thermal generation and rewards RES infeed over K time steps. Specifically, we define

$$J\left((x_0, \Delta_{-1}), (u, \Delta)|_{[0,K-1]}, w|_{[0,K-1]}\right) =$$

$$\sum_{k=0}^{K-1} \gamma^k \Big(\mathbf{1}_g^T P_{\mathcal{G}}(k) - \mathbf{1}_r^T P_{\mathcal{R}}(k) + C_{\mathcal{E}}^T |P_{\mathcal{E}}(k)| +$$

$$C_{on}^T \Delta(k) + C_{sw}^T |\Delta(k) - \Delta(k-1)| \Big), \quad (13)$$

where $C_{\mathcal{E}}^T |P_{\mathcal{E}}(k)|$, $C_{\mathcal{E}} \in \mathbb{R}_{0+}^e$ represents the cost for power transport which is assumed to increase linearly with the line length and the power transmitted over the line as in Adams and Laughton (1974). The power independent losses of the running machines are taken into account by the heuristic factor $C_{on} \in \mathbb{R}_{0+}^{(g+s+r)}$ and the switching costs by $C_{sw} \in \mathbb{R}_{0+}^{(g+s+r)}$. The past discrete state Δ_{-1} is needed to determine these costs for $k = 1$. The discount factor γ^k, $\gamma \in (0, 1]$ is introduced to emphasise performance in the near future over long-term performance. This is due to the increasing uncertainty in the long run. The corresponding OCP reads as follows.

Problem 1. (MPC). Find the optimal control input $(u, \Delta)|_{[k,k+K-1]}^*$ minimising

$$J\left((x_k, \Delta_{k-1}), (u, \Delta)|_{[k,k+K-1]}, w|_{[k,k+K-1]}\right)$$

subject to (4), (6), (8), (9), (10), (11) and (12).

To take into account uncertainties, only the current initial input, i.e. $u(k)$, $\Delta(k)$, is applied, and the Problem 1 is solved repetitively at time instant $k+1$. Clearly, this leads to a receding horizon control scheme.

3. SOLUTION

Problem 1 represents a hybrid dynamic programming problem with a polytopic disturbance. Solving such tasks is computationally highly nontrivial. A straightforward approximation is obtained by using the certainty equivalent (CE) assumption of a perfect disturbance prediction.

3.1 Certainty equivalent MPC

Assuming that the disturbance of the load and the renewable power output are known in advance, the polytopic hybrid MPC reduces to a hybrid MPC. A typical choice for such a disturbance would be the mean of the predicted upper and lower bound, i.e.

$$w(k) = \bar{w}(k) = \tfrac{1}{2}\left(w^{\max}(k) + w^{\min}(k)\right).$$

Then, the problem reduces as follows.

Problem 2. (Certainty equivalent MPC). Find the optimal control input $(u, \Delta)|_{[k,k+K-1]}^*$ minimising

$$J\left((x_k, \Delta_{k-1}), (u, \Delta)|_{[k,k+K-1]}, \bar{w}(k)|_{[k,k+K-1]}\right)$$

subject to (4), (8), (9), (10), (11) and (12).

The resulting MPC problem can be solved as a MILP as shown by Bemporad and Morari (1999). However, a satisfactory solution for the certainty equivalent (CE) MPC can be expected only for a reliable disturbance model. As good disturbance models are, in general, hard to obtain and possible deviations are not explicitly taken into account, the resulting controller may cause a violation of critical or physical constraints, potentially resulting in an unsafe operation. This motivates the integration of the disturbance bounds in the optimisation procedure leading to a minimax MPC framework explained in the following.

3.2 Minimax MPC

To provide a minimax formulation, we first need to analyse the impact of the uncertainty on the OCP. For each time instant k the load is assumed to lie in the forecast interval

$$\hat{w}_{\mathcal{L}}^{\min}(k) \leq w_{\mathcal{L}}(k) \leq \hat{w}_{\mathcal{L}}^{\max}(k) \tag{14a}$$

where $\hat{w}_{\mathcal{L}}^{\min}(k)$, $\hat{w}_{\mathcal{L}}^{\max}(k) \in \mathbb{R}^l$. The interval borders can be easily incorporated into the optimisation procedure.
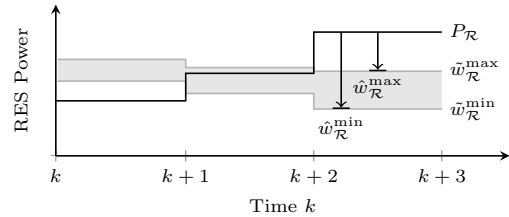

Fig. 1. Different cases for RES infeed and disturbance

In contrast, the perturbation corresponding to the RES is more challenging. Clearly, the fluctuation of the RES has an impact on the physically possible infeed $P_{\mathcal{R}}(k)$. In order to be able to treat $P_{\mathcal{R}}(k)$ as a bounded input variable, we assume that the RES disturbance is a function of the inputs, i.e.

$$\hat{w}_{\mathcal{R}}^{\min}(k,u) \leq w_{\mathcal{R}}(k,u) \leq \hat{w}_{\mathcal{R}}^{\max}(k,u). \tag{14b}$$

As the RES infeed is bounded, the perturbation will always be negative, resulting in the bounds

$$\hat{w}_{\mathcal{R}}^{\min}(k,u) = \begin{cases} \tilde{w}_{\mathcal{R}}^{\min}(k) - P_{\mathcal{R}}(k) & \text{if } \tilde{w}_{\mathcal{R}}^{\min}(k) \leq P_{\mathcal{R}}(k) \\ 0 & \text{else} \end{cases}$$

and

$$\hat{w}_{\mathcal{R}}^{\max}(k,u) = \begin{cases} \tilde{w}_{\mathcal{R}}^{\max}(k) - P_{\mathcal{R}}(k) & \text{if } \tilde{w}_{\mathcal{R}}^{\max}(k) \leq P_{\mathcal{R}}(k) \\ 0 & \text{else,} \end{cases}$$

where $\tilde{w}_{\mathcal{R}}^{\max}(k)$, $\tilde{w}_{\mathcal{R}}^{\min}(k) \in \mathbb{R}^r$ are the predicted values for the maximum and minimum RES infeed.

The possible scenarios for the bounds are depicted in Fig. 1 over three time instants. Between k_0 and k_1, the maximum $\tilde{w}_{\mathcal{R}}^{\max}$ and minimum $\tilde{w}_{\mathcal{R}}^{\min}$ predicted infeed lie above the limitation $P_{\mathcal{R}}(k)$. As the RES infeed in this case can be guaranteed, the disturbances $\hat{w}_{\mathcal{R}}^{\min}$ and $\hat{w}_{\mathcal{R}}^{\max}$ are zero. From k_1 to k_2, the set point of $P_{\mathcal{R}}(k)$ lies between the bounds of the predicted RES infeed. Thus, the upper perturbation limit $\hat{w}_{\mathcal{R}}^{\max}(k,u)$ can be set to zero as no

power bigger than $P_{\mathcal{R}}(k)$ will appear, while the lower disturbance limit is given by the difference between $\tilde{w}_{\mathcal{R}}^{\min}(k)$ and $P_{\mathcal{R}}(k)$. If $P_{\mathcal{R}}(k)$ is above the predicted $\tilde{w}_{\mathcal{R}}^{\max}$, the corresponding limits are $\hat{w}_{\mathcal{R}}^{\min}(k,u) = \tilde{w}_{\mathcal{R}}^{\min}(k) - P_{\mathcal{R}}(k)$ and $\hat{w}_{\mathcal{R}}^{\max}(k,u) = \tilde{w}_{\mathcal{R}}^{\max}(k) - P_{\mathcal{R}}(k)$. In this case only negative perturbations will be present. This is very common in grids with a small amount of installed RES facilities, if the infeed is not limited.
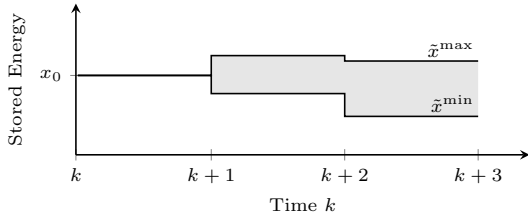
Fig. 2. Bounds for the storage level in minimax MPC

The evolution of the storage levels depends directly on the disturbances. Therefore, only an upper and a lower limit for the evolution of $x(k)$ can be derived by modifying (9). The lower bound of the storage level $\tilde{x}^{\min}(k) \in \mathbb{R}_{0+}^s$ is described by

$$\tilde{x}^{\min}(k+1) = \mathbf{A}\tilde{x}^{\min}(k) + \mathbf{B}\big(u(k) + \mathbf{H}(\Delta)\hat{w}^{\min}(k,u)\big)$$
$$\tilde{x}^{\min}(0) = x_0 \quad (15a)$$

and the upper level $\tilde{x}^{\max}(k) \in \mathbb{R}_{0+}^s$ by

$$\tilde{x}^{\max}(k+1) = \mathbf{A}\tilde{x}^{\max}(k) + \mathbf{B}\big(u(k) + \mathbf{H}(\Delta)\hat{w}^{\max}(k,u)\big)$$
$$\tilde{x}^{\max}(0) = x_0. \quad (15b)$$

The initial states $\tilde{x}^{\min}(0)$ and $\tilde{x}^{\max}(0)$ are always equivalent, while the bounds diverge over time, as shown in Fig. 2. Note that the limits of the storage (10) still hold for the corresponding values of $\tilde{x}^{\min}(k)$ and $\tilde{x}^{\max}(k)$. Therefore, it has to be assured that

$$x^{\min} \leq \tilde{x}^{\min}(k) \leq \tilde{x}^{\max}(k) \leq x^{\max}. \quad (16)$$

Note that the CE case, treated in the previous subsection is also included. The corresponding minimax OCP reads as follows.

Problem 3. (Minimax MPC). Find the optimal control input $(u,\Delta)|_{[k,k+K-1]}^*$ minimising

$$\max_w J\big((x_k,\Delta_{k-1}),(u,\Delta)|_{[k,k+K-1],\Delta_k},w|_{[k,k+K-1]}\big)$$

subject to (4), (8), (11), (12), (14), (15) and (16).

This problem can be formulated as a MILP in a similar way as proposed by Bemporad et al. (2003) and solved numerically online. Now we want to compare both approaches in a numerical case study of a microgrid.

4. CASE STUDY

In the following exemplary case study, the MG is assumed to be operated in island mode. This is the more ambitious task compared to on-grid operation, as the storage and thermal generation have to cover all variations in load and RES infeed on their own. Throughout this section, all values are normed to one power unit of 1 pu and a time of 1 h for convenience.

The microgrid structure shown in Fig. 3 is used in our case study. It consists of a load $w_{\mathcal{L}}(k) \in \mathbb{R}$, a RES $P_{\mathcal{R}}(k) \in \mathbb{R}_{0+}$, a storage device $P_{\mathcal{S}}(k) \in \mathbb{R}$ and a
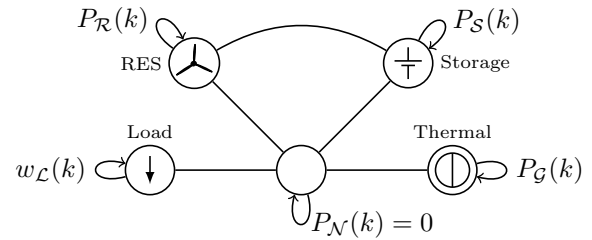

Fig. 3. Exemplary microgrid

thermal generator $P_{\mathcal{G}}(k) \in \mathbb{R}_{0+}$. Hence, $x(k) \in \mathbb{R}_{0+}$, $\Delta(k) \in \mathbb{B}^3$, $u(k) = (P_{\mathcal{G}}(k), P_{\mathcal{S}}(k), P_{\mathcal{R}}(k))^T \in \mathbb{R}^3$, $w(k,u) \in \mathbb{R}^2$ and $P_{\mathcal{E}}(k) \in \mathbb{R}^5$. The corresponding limits for the devices are assumed as $(x^{\min}, x^{\max}) = (0.167, 0.833)$, $u^{\min} = (0.5, -0.9, 0)^T$, $u^{\max} = (0.9, 0.9, 2)^T$, the line limits as $(P_{\mathcal{E}}^{\min}, P_{\mathcal{E}}^{\max}) = \mathbf{1}_5 \cdot (-1.3, 1.3)$ and the ancillary service as $P_{\mathcal{U}}^{sc} = (1, 1, 0.2)$ and $p^{sc} = 1$. A sampling time of $t_S = 1/6$ h, resulting in $\mathbf{B} = -(0, 1/6$ h$, 0)$ and $\mathbf{A} = 1$ were assumed.
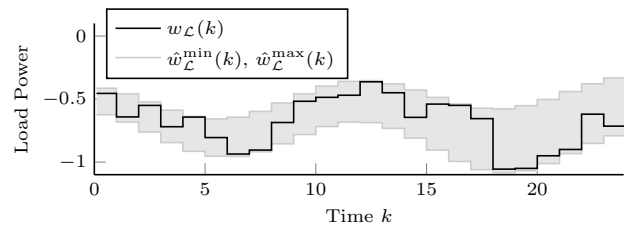

Fig. 4. Load over time with predicted bounds

An optimisation horizon of $K = 6$ was chosen. The resulting MPC schemes were implemented for a simulation scenario of 4 h, i.e. $k \in [0, 23]$. The problem was formulated as a MILP, using Yalmip (Löfberg (2004)) in MATLAB®, and solved with CPLEX. Solving the problem for one time instant took less than 1 s for both the CE and the MM MPC, with an Intel® Core™ i5-3320M processor @ 2.6 GHz with 8 GB of RAM, which is very short compared to the sampling interval of 1/6 h.
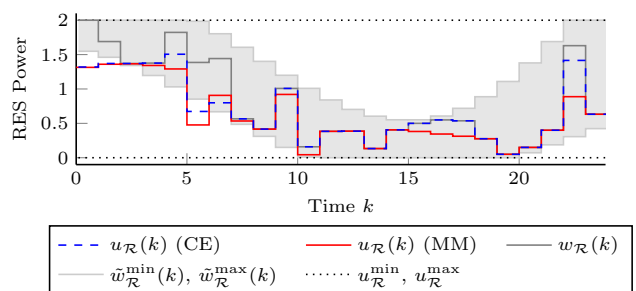

Fig. 5. RES infeed over time

The load profile in Fig. 4 was used for the simulation. The MM only needs the bounds of the load and the CE MPC uses the mean of the disturbance. The real load is denoted by $w_{\mathcal{L}}(k)$. The forecast of the RES infeed is given by the bounds $\tilde{w}_{\mathcal{R}}^{\min}(k)$ and $\tilde{w}_{\mathcal{R}}^{\max}(k)$ for the MM and by the mean for the CE MPC. Note that the predicted RES infeed is limited by the hard constraints $u_{\mathcal{R}}^{\min}$ and $u_{\mathcal{R}}^{\max}$. In both solutions the RES is limited, due to limits of other machines, especially the storage device (e.g. $u_{\mathcal{S}}(k)$ for $k \in [1, 5]$).
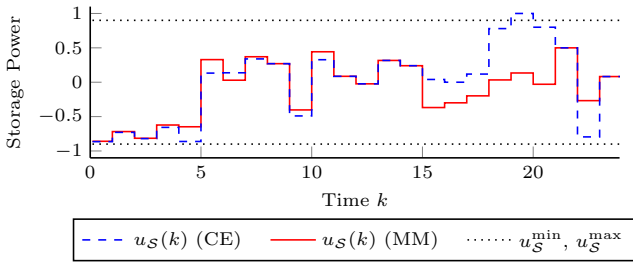
Fig. 6. Optimised control input $u_{\mathcal{S}}(k)$, limits $u_{\mathcal{S}}^{\min}$, $u_{\mathcal{S}}^{\max}$

As seen in Fig. 6, applying the CE MPC leads to a violation of the power limits at $k = 19$ as the forecast uncertainty in not taken into account. Also the bounds of the stored energy are violated at $k = 5$ and $k = 22$, when using a CE approach. Using the MM MPC, these limits are not violated, but the RES infeed is lower due to the inherent conservativeness of the approach, as seen in Fig 5.
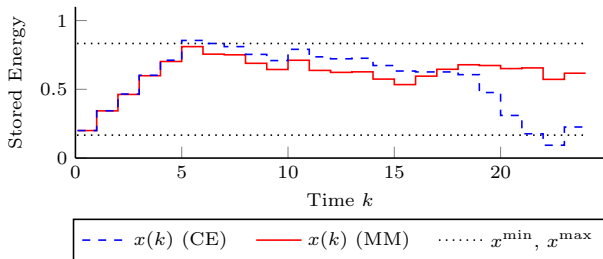

Fig. 7. State $x(k)$ with limits $x^{\min}$ and $x^{\max}$

The thermal generator is turned on (because of the forecasts) from $k = 15$ to $k = 21$ in Fig. 8 to prevent a violation of the storage power limits by the load. In this time the variation in power is shared among the storage device and the thermal generator.
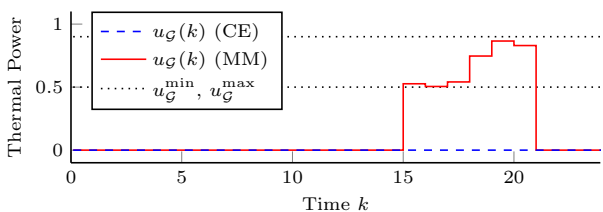

Fig. 8. Optimal control input $u_{\mathcal{G}}(k)$, limits $u_{\mathcal{G}}^{\min}$, $u_{\mathcal{G}}^{\max}$

To compare the two operational strategies, when running the grid with the disturbances, the costs for $C_{\mathcal{E}} = 0.1 \cdot \mathbf{1}_5$, $C_{on} = 0.1 \cdot \mathbf{1}_3$, $C_{SW} = 0.2 \cdot \mathbf{1}_3$, $\gamma = 0.9$, $x_0 = 0.2$ and $\Delta_0 = \mathbf{0}_3$ are calculated. As the RES infeed is lower and the thermal unit is switched on, when operated with the MM MPC, the costs for this case $J_{MM}^* = 3.11$ are higher than with the CE MPC, where $J_{CE}^* = -2.76$. In exchange, the constraints are not violated, when operating the microgrid with the MM MPC.

5. CONCLUSIONS

This paper studied the model predictive operation control of microgrids in islanded operation mode. A novel problem was introduced, where the power infeed of the renewable sources can be curtailed in order to keep the electrical equipment in its limits. The resulting problem was solved

in a robust way in order to cope with the uncertainties of the load and the renewable generation. In the provided numerical case study, the proposed control provides a good alternative to the widely used certainty equivalent solution and keeps the system within the bounds. Future work will address the optimal operation control of MG in a closed loop minimax or a probabilistic manner to obtain less conservative estimates and increase the RES infeed.

REFERENCES

Adams, R. and Laughton, M. (1974). Optimal planning of power networks using mixed-integer programming. part 1: Static and time-phased network synthesis. *Proc. of the Inst. of Electrical Engineers*, 121(2), 139–147.

Arnold, M., Negenborn, R., Andersson, G., and Schutter, B.D. (2009). Multi-area predictive control for combined electricity and natural gas systems. In *2009 IEEE ECC*.

Bemporad, A., Borrelli, F., and Morari, M. (2003). Minmax control of constrained uncertain discrete-time linear systems. *IEEE Trans. on Automatic Control*, 48(9), 1600–1606.

Bemporad, A. and Morari, M. (1999). Control of systems integrating logic, dynamics, and constraints. *Automatica*, 35(3), 407–427.

Bertsimas, D., Litvinov, E., Sun, X.A., Zhao, J., and Zheng, T. (2013). Adaptive robust optimization for the security constrained unit commitment problem. *IEEE Trans. on Power Systems*, 28, 52–63.

Heussen, K., Koch, S., Ulbig, A., and Andersson, G. (2010). Energy storage in power system operation: The power nodes modeling framework. In *2010 IEEE PES ISGT Europe*, 1–8.

Jiang, R., Wang, J., Zhang, M., and Guan, Y. (2013). Two-stage minimax regret robust unit commitment. *IEEE Trans. on Power Systems*, 28(3), 2271–2282.

Löfberg, J. (2004). Yalmip: A toolbox for modeling and optimization in matlab. In *13th IEEE CACSD*, 284–289.

Lopes, J., Moreira, C., and Madureira, A. (2006). Defining control strategies for microgrids islanded operation. *IEEE Trans. on Power Systems*, 21(2), 916–924.

Parisio, A. and Glielmo, L. (2011). Energy efficient microgrid management using model predictive control. In *50th IEEE CDC and ECC*, 5449–5454.

Purchala, K., Meeus, L., Van Dommelen, D., and Belmans, R. (2005). Usefulness of dc power flow for active power flow analysis. In *2005 IEEE PES General Meeting*, 454–459. IEEE.

Schiffer, J., Anta, A., Trung, T., Raisch, J., and Sezi, T. (2012). On power sharing and stability in autonomous inverter-based microgrids. In *51st IEEE CDC*, 1105–1110.

Zafra-Cabeza, A., del Real, A., Arce, A., Camacho, E., Ridao, M., and Bordons, C. (2010). A risk-based strategy for power system optimization. In *49th IEEE CDC*, 1905–1910.

Zhao, C. and Guan, Y. (2013). Unified stochastic and robust unit commitment. *IEEE Trans. on Power Systems*, 28(3), 3353–3361.